Wide-bandwidth drift-scan pulsar surveys of globular clusters: application to early science observations with FAST

2016 Res. Astron. Astrophys. 16 151

(http://iopscience.iop.org/1674-4527/16/10/151)

RAA 2016 Vol. **16** No. **10**, 151 (10pp) doi: 10.1088/1674–4527/16/10/151
http://www.raa-journal.org *http://iopscience.iop.org/raa*

***R**esearch in*
***A**stronomy and*
***A**strophysics*

Wide-bandwidth drift-scan pulsar surveys of globular clusters: application to early science observations with FAST

Lei Zhang[1,2], George Hobbs[3,2], Di Li[2,4], Duncan Lorimer[5,6], Jie Zhang[1], Meng Yu[2], You-Ling Yue[2], Pei Wang[2], Zhi-Chen Pan[2] and Shi Dai[3]

[1] School of Physics and Space Science, China West Normal University, Nanchong 637002, China; *leizhang996@nao.cas.cn*
[2] National Astronomical Observatories, Chinese Academy of Sciences, Beijing 100012, China
[3] Australia Telescope National Facility, CSIRO, PO Box 76, Epping NSW 1710, Australia
[4] Key Laboratory of Radio Astronomy, Chinese Academy of Sciences, Nanjing 210008, China
[5] Department of Physics and Astronomy, White Hall, West Virginia University, Morgantown, WV 26506, USA
[6] National Radio Astronomy Observatory, Green Bank Observatory, PO Box 2, Green Bank, WV 24944, USA

Received 2016 February 5; accepted 2016 May 20

Abstract The Five-hundred-meter Aperture Spherical Telescope (FAST) will begin its early-science operations during 2016. Drift-scan pulsar surveys will be carried out during this period using an ultra-wide-band receiver system (covering ~ 270 to 1620 MHz). We describe a method for accounting for the changes in the telescope beam shape and the pulsar parameters when searching for pulsars over such a wide bandwidth. We applied this method to simulated data sets of pulsars in globular clusters that are visible to FAST and found that a representative observation would have a sensitivity of ~ 40 μJy. Our results showed that a single drift-scan (lasting less than a minute) is likely to find at least one pulsar for observations of four globular clusters. Repeated observations will increase the likely number of detections. We found that pulsars in ∼16 clusters are likely to be found if the data from 100 drift-scan observations of each cluster are incoherently combined.

Key words: pulsars — drift-scan pulsar surveys — globular clusters

1 INTRODUCTION

The ATNF Pulsar Catalogue[1] (e.g. Manchester et al. 2005) lists more than 2400 currently known radio pulsars. Even though the majority of these pulsars reside in our Galaxy, 28 pulsars have been discovered in the Magellanic Clouds and more than 144 pulsars are associated with globular clusters (GCs). Most pulsar surveys belong to one of three categories: "large-area pointed surveys" (e.g. Manchester et al. 2001) in which an extensive region of the sky is surveyed by making many individual observations, "drift-scan surveys" (e.g. Hessels et al. 2008; Deneva et al. 2013) in which the telescope remains pointing in one direction and surveys any sky that passes through the beam and "targeted surveys" (e.g. Manchester et al. 1982) in which the telescope observes objects that are likely to contain pulsars such as supernova remnants, high-energy sources, GCs, and/or nearby galaxies.

The Five-hundred-meter Aperture Spherical Telescope (FAST) is expected to revolutionise pulsar astronomy (e.g. Nan et al. 2011). It will be the world's largest single dish radio telescope and will be equipped with a suite of modern receivers. FAST should provide the highest quality pulsar profile observations and pulsar timing data, which will have profound impacts on various fields of astrophysics. For instance, Hobbs et al. (2014) described how FAST observations will be used in the search for ultra-low-frequency gravitational waves.

FAST will also discover new pulsars. Smits et al. (2009) considered two surveys with FAST. The first was a search for pulsars in the Galactic plane. They assumed eight hours of observing per day over 200 days. Such a survey, using a 19-beam focal plane feed-horn array operating in the 20 cm band, was expected to discover ∼5200 currently unknown pulsars in the Galactic plane, including ∼460 millisecond pulsars (MSPs). Smits et al. (2009) also considered a search for extragalactic pulsars in M31 and M33. They showed that 470 hours of observing with a 19-beam receiver would lead to between 50 and 100 new pulsar discoveries. Yue et al. (2013) considered a drift-scan pulsar survey using a low frequency (∼400 MHz) 7-beam receiver system. Such a survey was expected to discover ∼1500 new normal pulsars and about 200 MSPs.

The multibeam receiver systems described above will not be available for the very first science observations with FAST (expected late in 2016). Instead, the first observa-

[1] *http://www.atnf.csiro.au/research/pulsar/psrcat*

tions will be made using a single beam, ultra-wide bandwidth receiver system with a frequency range between 270 and 1620 MHz and a receiver temperature of ∼35 K across most of the band. As described in this paper, carrying out a pulsar survey with such a large bandwidth provides many opportunities, but also leads to many challenges.

Early FAST observations will be carried out as drift-scans because of the need to minimise (for, at least, the first few months of observations) attrition of the actuator system and expected radio frequency interference (RFI) from moving the hydraulic systems. Until these issues have been properly dealt with, observers will be required to move the telescope pointing position to a specific part of the sky and then let the sky drift through the beam. As this is not a common observing mode and was not considered in the earlier publications relating to FAST surveys, it is now essential that we determine how best to carry out a drift-scan survey with an ultra-wide-band receiver system and to determine the expected number of pulsar discoveries that will be made during this early science period. The results from our analysis are presented in this paper. Even though our paper is based on an analysis of pulsar surveys using the FAST telescope, most major radio observatories are now using or commissioning ultra-wide-band receiver systems. Our analysis methods are applicable to any wide-bandwidth pulsar survey.

In this paper, we first describe a new method to optimise the detectability of a pulsed signal in a wide-bandwidth drift-scan survey. In Section 2, we describe the early science systems for FAST and demonstrate how FAST observations can be simulated. In Section 3, we discuss the expected survey sensitivity for early pulsar surveys with FAST and demonstrate how the sensitivity will increase with multiple observations of the same source. In Section 4, we apply our results to searches for pulsars in GCs. We conclude in Section 5.

2 WIDE-BAND, DRIFT-SCAN SURVEYS

The sensitivity of any pulsar survey is a function of many factors including the receiver and sky background noise temperatures, the antenna gain, the observing bandwidth and observing time, the pulse period and its dispersion measure, the pulse duty cycle, data digitization effects, processing algorithms and interference levels. An estimate of the minimum detectable flux density for a pointed pulsar survey is given by (e.g. Lorimer & Kramer 2004)

$$S_{\rm min} = \frac{\alpha\beta T_{\rm sys}}{G(N_p \Delta\nu T_{\rm int})^{1/2}} \left(\frac{W}{P-W}\right)^{1/2}, \qquad (1)$$

where $T_{\rm sys}$ is the system temperature, G the telescope gain, N_p the number of summed polarisations, $\Delta\nu$ the observing bandwidth, $T_{\rm int}$ the integration time, P the pulse period and W the pulse width. α is the minimum signal-to-noise ratio (S/N) required to detect a source and β is a factor that is close to unity and represents digitization and other processing effects.

For a drift-scan survey the S/N of any individual source will be changing as a function of time. For a wide-band system many other parameters will be changing as a function of the observing frequency. These include parameters relating to the system and the noise levels, such as the receiver and sky temperatures, the intrinsic properties of the pulsar itself, such as its spectral index and pulse width, and phenomena caused by the interstellar medium, such as pulse dispersion, scintillation and scattering.

Pulsar survey data sets are recorded as follows:

- The signal from the telescope is channelised into $N_{\rm chan}$ frequency channels evenly spaced through the observing band.
- The signal in each channel is recorded (usually with 1, 2, 4 or 8 bit precision) with a sampling time of ΔT.
- These data are archived.

Each data file is then processed with a software pipeline that usually:

- dedisperses the data in each frequency channel in a range of trial dispersion measures;
- sums the frequency channels in the dedispersed time series to form a single time series for each trial dispersion measure;
- Fourier transforms each trial time series and searches for significant periodicities;
- iterates the above steps to find optimised solutions for period and dispersion measure;
- records these periodicities and the corresponding dispersion measures as possible pulsar candidates.

Throughout this paper we make use of the SIGPROC software[2] package (e.g. Lorimer 2001). After Fourier transforming the dedispersed, single frequency time series, SIGPROC forms an amplitude spectrum that has been normalised to give a root mean square (rms) of 1. The S/N of a particular spectral channel is its normalised amplitude divided by the local rms value. SIGPROC also attempts to improve the sensitivity to narrow pulses by a process known as harmonic summing. For each harmonic folding the rms values are scaled up by $\sqrt{2}$. The cut-off S/N for a likely pulsar candidate depends upon the number of spectral channels and the number of trial dispersion measures (DMs). We discuss this for FAST later, but, for most of this paper, take a nominal cut-off value of $\alpha = 8$.

2.1 Early Science Systems for FAST

The methods described in this section can be applied to any telescope system. We focus here on the expected capabilities of FAST for its early science. The telescope size, position and declination range are given in Table 1. The parameters for the ultra-wide band receiver system and the corresponding backend are also listed in the table. It is unlikely that the entire band will be recorded. Even though the telescope site is relatively quiet, significant RFI is known to exist around 900 MHz. Throughout this paper we therefore

[2] *http://sigproc.sourceforge.net*

consider a low-band and a high-band that are divided by the known, strong RFI. These bands are parameterised in Table 2.

It will not be possible to centre the received signal frequency in the middle of band 1. Instead the backend will provide up to 8192 frequency channels over a band from 0 to 910 MHz. The data between 0 and 270 MHz and from ∼850 to 910 MHz will be unusable. The former are due to the receiver cutoff and the latter to the RFI environment. It is likely that the complete 910 to 1820 MHz band can be recorded with the full 8192 channels giving around 5850 channels in the observing band between 970 and 1620 MHz. The pulsar and interstellar medium properties can significantly change across such wide bands. We therefore find it useful to divide each of these two observing bands into two sections. We thus have:

- band 1a: from 270 to 560 MHz with up to 2610 channels
- band 1b: from 560 to 850 MHz with up to 2610 channels
- band 2a: from 970 to 1295 MHz with up to 2925 channels
- band 2b: from 1295 to 1620 MHz with up to 2925 channels

2.2 Simulating a Wide-bandwidth, Drift-scan Data Set

In order to demonstrate and test our algorithms we simulated pulsar search data sets. Our code assumes a perfect pulse train with an unchanging pulse period and identical individual pulses[3]. Each pulse has, prior to dispersion smearing or scattering effects, a Gaussian form and we assumed white, Gaussian radiometer noise. Our simulations account for the expected beam shape, the receiver noise and pulse dispersion. The sky temperature is modelled as

$$T_{\rm sky}(f) = T_0 \left(\frac{f}{f_0}\right)^{-2.6}, \qquad (2)$$

where T_0 is the measured sky temperature in the specified sky position at a frequency of f_0, estimated from an all-sky continuum survey (e.g. Haslam 1985). Over a small band, or at high frequencies, the changes in $T_{\rm sky}$ over the band are usually negligible and ignored. However, for a wide-band survey it is necessary to account for the changing system temperature. The pulse flux density is assumed to follow a power law

$$S(f) = S_0 \left(\frac{f}{f_0}\right)^{\gamma}, \qquad (3)$$

where S_0 is the flux density measured at frequency f_0. The spectral index, γ, can be modified by the user, but for this work is assumed to be -1.4 (e.g. Bates et al. 2013). The intrinsic pulse width is assumed to remain constant with frequency, but the measured pulse width will change because of scattering and dispersion smearing. Dispersion smearing is simulated by modelling the pulse shape with a much finer channel bandwidth than the user requested. The final output is summed over the fine channels to give the number of channels that was requested. The simulations produce either filterbank files or a single, dedispersed time series in the SIGPROC filterbank format and therefore can be processed using the standard pulsar search pipelines. The simulation software is available for download in a git repository hosted by *https://bitbucket.org/psrsoft/simpulsetrain*.

[3] We are currently updating the software package to allow the individual pulses to vary in order to study pulse flux density distributions, nulling and sub-pulse drifting. Such extensions to the software will be described elsewhere and do not affect the results of this paper.

2.3 Channel Weighted Dedispersion

For simplicity, we assume that the beam shape can be described as a sinc^2 function in which the first null occurs at $1.22\lambda/D$ where D is the effective telescope diameter and λ is the observing wavelength. However, we note that the following analysis can be generalised to any beam shape.

The exact beam shape will depend upon the receiver itself and tapering effects. We can write the receiver gain for a particular source as a function of the angular offset between the pointing direction and the source and also of the observing frequency, $G(\theta, \nu)$. The time any particular source remains in the beam depends upon the cosine of the source declination and the beam shape. As an example we show, in Figure 1, a simulated data set. We simulated a pulsar with a pulse period of 5 ms, a pulse width of 5% of the period, a DM of 30 cm^{-3} pc and a declination angle of 45°. For T_0 and f_0 in Equation (2) we chose 30 K and 430 MHz respectively. For this simulation we include the effect of dispersion smearing within each frequency channel, but do not simulate scattering. The left panels show simulated data in band 1a. The right panels show simulated data in band 2b. In all of the panels the individual pulses have been folded to produce an individual pulse profile. The pulse intensity is indicated using the colour scale.

In the top panels we indicate how the pulse intensity varies with time. Over the simulated 20 seconds the pulse remains almost constant in the lowest band, but the beam shape is detectable in the high-frequency band. The bottom panels show the pulse profile as a function of observing frequency. The sky noise temperature increases as the observing frequency decreases whereas the pulsar's flux density increases. In the high-frequency band, very little change is detectable across the band. In the low-frequency band, the variation across the band becomes very noticeable because of the dispersion smearing.

For the FAST band 1a the drift time will be ~ 68 seconds (at 270 MHz) whereas a source will drift through the beam in band 2b in only $\sim$ 11 s (at 1620 MHz). If the observer chooses to observe for 60 s then the pulsed signal will be undetectable during most of the observation in the high band, whereas if the observer only chooses to observe for $\sim$ 10 s then the sensitivity at low frequencies will be reduced. Hence, if the observer wishes to maximise the survey sensitivity it is necessary to weight the data in each frequency channel by the beam shape for obtaining the frequency-summed, dedispersed time series. For sample j, in observing frequency channel i, we can use the

Table 1 The Basic Parameters for FAST and Its Initial Pulsar Observing System

Telescope	
Size (m)	500
Effective size (m)	300
Site coordinates	(25.7° N, 106.9° E)
Declination range	$-14°$ to $+66°$
Observation type	drift-scan
Receiver	
Receiver temperature (K)	35
Number of beams	1
Polarizations	2
Telescope gain (K Jy^{-1})	16
Band range (MHz)	270–1620
Backend	
Maximum number of channels	0–910 (8192), 910–1820 (8192)
Maximum sampling time (μs)	50

Table 2 Expected Observing Bands Available for Early FAST Science Observations

	Band 1	**Band 2**
Frequency range (MHz)	270 to 850	970 to 1620
Bandwidth (MHz)	580	630
Available channels across the band	5220	5850
Central frequency (MHz)	560	1295
Central half-power beamwidth (arcmin)	6.2	2.7
Approximate drift time (s)	33	14

following, very simple, weighting

$$X'_{ij} = X_{ij} G(\nu_i, \theta_j). \quad (4)$$

Throughout this paper we assume that the drift-scan leads to variations in the telescope gain that follows[4]

$$G(\nu_i, \theta_j) = \left[\frac{\sin \zeta_{ij}}{\zeta_{ij}}\right]^2 \quad (5)$$

where ζ_{ij} is a function of time and observing frequency. This is set so that the first null in $G(\nu_i, \theta_j)$ occurs at $1.22\lambda/D$ where $\lambda = c/\nu_i$ and D is the telescope diameter. To convert this angular function into a drift time we scale by $\cos(\delta)$ where δ is the declination of the source.

It would be straightforward to update the SIGPROC software to include this weighting during the dedispersion stage. However, we have included a dedispersion routine in our simulation software that can account for the weighting. The simulation software therefore outputs a file containing all the filterbank channels without dedispersion and another, much smaller, file that has been weighted, dedispersed and summed across the frequency channels. To demonstrate the effectiveness of the weighting, we simulated a 2 minute drift-scan observation in band 2b, but for simplicity we only simulated 32 frequency channels. We simulated a pulsar with a period of 0.5 s, a width of 5% of the period and a dispersion measure of 30 cm^{-3} pc. A pulse flux density of 0.2 mJy led to a SIGPROC S/N of 15. After weighting the dedispersed time series, the S/N value increased to 32. Of course, the improvement in S/N depends upon the chosen band and the integration time.

3 THE EXPECTED SURVEY SENSITIVITY FOR EARLY PULSAR SURVEYS WITH FAST

In order to determine the expected survey sensitivity with FAST for different types of pulsars, we simulated data sets in which each pulsar has a specific pulse period, P, a position in Galactic coordinates and a DM. We assumed that the intrinsic pulse width $W = 0.05P$. We examined a wide range of pulse flux densities. For these datasets we provided the flux density for each simulated pulsar at 1400 MHz. The actual flux density used was scaled, using Equation (3), to the relevant observing frequency. For each trial we produced a weighted, dedispersed, frequency-summed time series. We then used the SIGPROC software to measure the S/N. We identified the flux density that gave an S/N close to our nominal cutoff value of 8. This procedure was repeated for different periods and/or dispersion measures.

These simulations gave results that are similar (for small periods) to analytic calculations based on Equation (1) (see also Zhang et al. 2015). However, for large pulse periods and short integration times the analytic equation breaks down[5].

[4] Of course, it is unlikely that the true beam shape will follow this expression exactly. During the early science commissioning period, the observers will make an exact measurement of the beam shape, and the weighting factors described in this paper can then be updated based on their results.

[5] Clearly a pulsar with a period of 8 s would not be detectable using a periodicity search in a short 10 s observation.

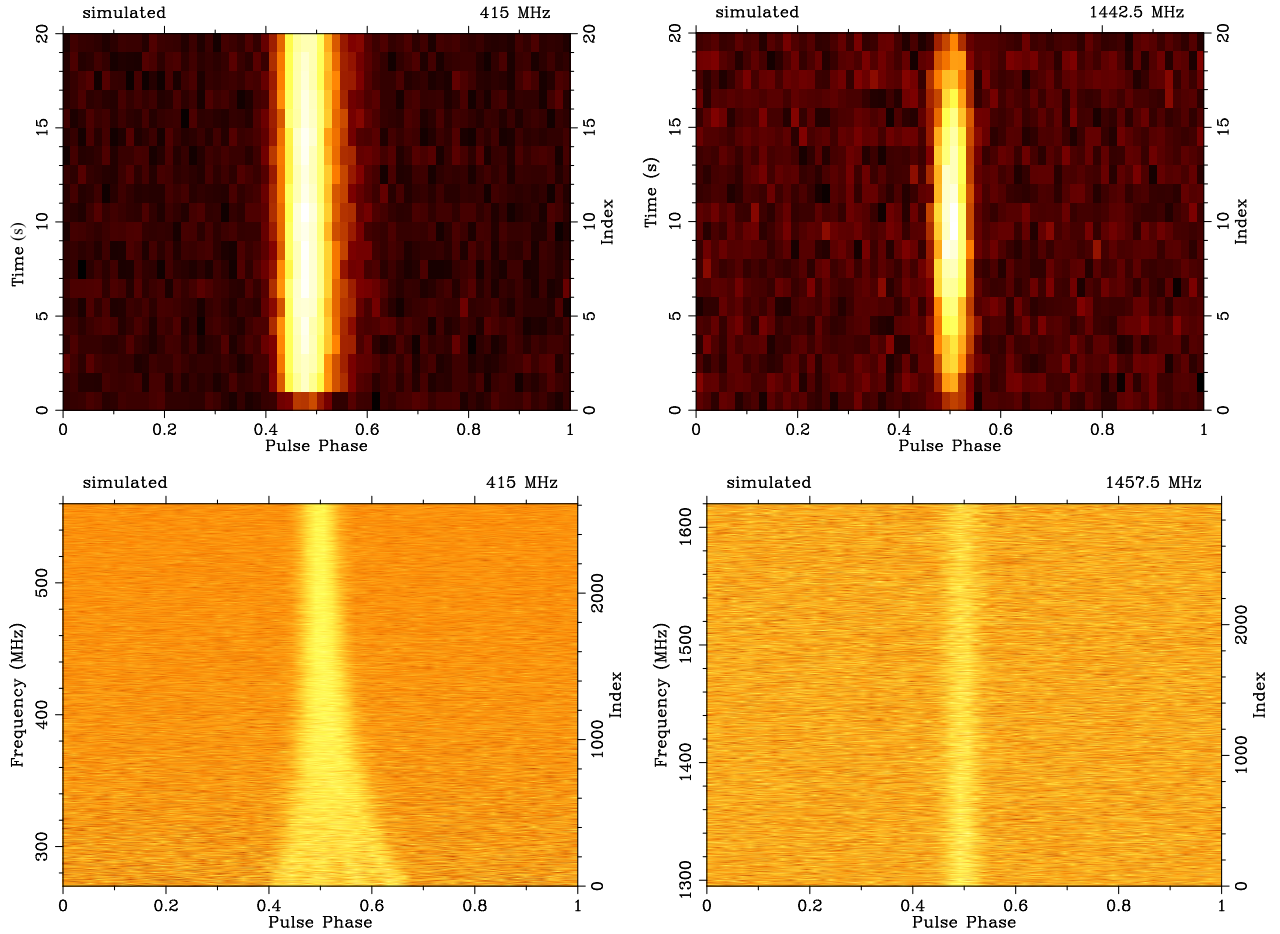

Fig. 1 Simulated data sets in the two bands of the FAST early-science receiver. The left panels show a simulated pulsar signal in the lowest observing band. The right panels are the same pulsar in the highest observing band. The top panels show the pulsed signal strength (colour scale) as a function of pulse phase and time. Note that the lack of signal in the first second of data in the top-left panel is an artefact caused by the dedispersion (the dispersion time is $\sim$1 s in this band. The bottom panels show the pulsed signal strength as a function of observing frequency across the band. The signal is dominated by inter-channel dispersion smearing and so scattering effects are not simulated for these figures.

In Figure 2 we show the expected survey sensitivity as a function of pulse period for different subbands and pulse periods. For the results of simulated band 1b, the sensitivity is given as the 1400 MHz sensitivity assuming a spectral index of -1.4. The blue dashed line is the scaled predicted sensitivity. The blue solid line is the predicted flux density sensitivity in the centre of the observing band (705 MHz) without any scaling. Note that the simulation sensitivity is around a factor of 2 worse than the analytic prediction. This is not surprising. The simulation data are processed using actual search software and, in contrast with the analytic calculation, the simulation accounts for the changes in signal strength caused by the drift-scan and changes in the noise properties and pulse flux density over the observing band. The magenta (dashed), green (dotted) and yellow (dot-dashed) lines give the analytic flux density sensitivity for the centre of bands 1a, 2a and 2b respectively. The solid lines theoretically extend to any large pulse period, but clearly a single pulse from a long-period pulsar would not be detectable using a periodicity pulsar search. We therefore cut the lines at a period corresponding to four pulses during the drift scan. For normal (i.e., non-MSPs) it is clear that the lowest frequency bands are the most sensitive to pulsars (away from the Galactic plane). Such pulsar surveys should be carried out in the low band with an observation time of $\sim$60 seconds. The lowest part of band 1 is unsuitable for searching for MSPs because of the dispersion smearing across each frequency channel. The ideal observing strategy for MSPs is therefore to make use of the high part of band 1 (e.g., band 1b) or the low part of band 2 (e.g., band 2a) depending on an estimate of the periods and DMs for the expected pulsars.

The open red circles in Figure 2 were obtained via simulation and are therefore affected by the number of realisations carried out. In order to consider this further we show, in Figure 3, more details of the simulations used to determine the sensitivity for a pulse period of 0.1 s. For a range of flux density values we create five simulated data sets. The S/N values of the pulsar as determined via SIGPROC are shown as open circles (red after using our weighting scheme and green for unweighted results). The averages of these data points are shown using the triangle symbols

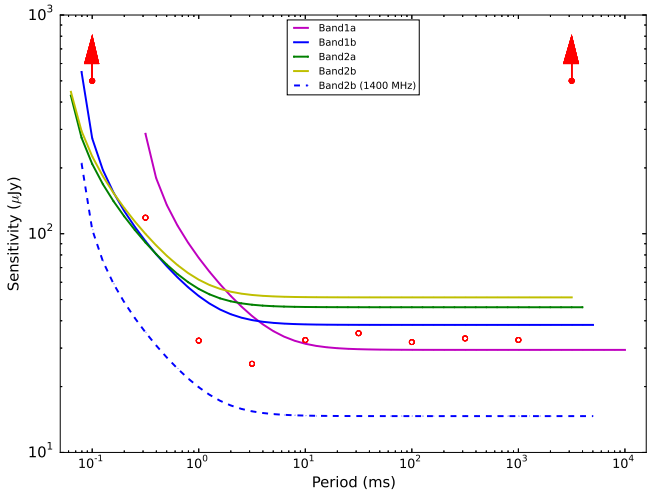

Fig. 2 The survey sensitivity for different observing bands assuming a pulsar with a DM of 20 cm^{-3} pc and a declination of 0°. The red circles give the survey sensitivity as obtained using our simulation software and the channel-weighted SIGPROC search pipeline in band 1b for a 30 s observation. The circles are direct measurements of the sensitivity whereas the red arrows indicate regions in which the simulated pulsar was undetectable at any flux density (and therefore represent lower limits to the true sensitivity). The blue solid line is the predicted, non-scaled flux density sensitivity in the centre of the 1b observing band. The magenta, green and yellow lines give the analytic predictions for bands 1a, 2a and 2b respectively. The observation durations were 60/30/20 and 15 s for the analytic determination in the four bands. The blue dashed line is the analytic sensitivity of observing band 1b scaled to a frequency of 1400 MHz.

(note for clarity the open circles are slightly offset from the actual flux value simulated). In the left panel we show the results for simulations of 30 s observations. In the right panel we show the same, but for 60 s observations. These results indicate, as expected, that the weighting becomes more important as the observing span increases.

The exact values for the limiting flux density as shown in Figure 2 were obtained by determining the flux density value which leads to a weighted S/N of 8. As shown in Figure 3 there is a small uncertainty on this value (typically < 10 μJy).

Discussing the survey sensitivity is non-trivial as it depends on the band chosen, the pulse period and the DM. The flux density results can also, if necessary, be scaled to the expected flux density at, e.g., 1400 MHz assuming a given spectral index. However, it is clear from Figure 2 that we can expect a limiting sensitivity of ~ 30 to 60 μJy. The drift-times will be short and therefore it is likely that many drift-scan observations will be taken for the same source. Ignoring pulse intensity variations caused by, e.g., scintillation, the survey sensitivity will scale with the number of drift-scan observations of the particular source as $\sqrt{N_{\mathrm{drift}}}$ after incoherently stacking the power spectra.

4 SEARCHING FOR PULSARS IN GCS

As shown in the previous section, we can estimate the sensitivity of a FAST drift-scan survey in a particular observing band and for a particular sky position. A drift-scan pointing directly upwards, or passing through a region of the Galactic plane may lead to the discovery of a few pulsars, but the FAST beam is narrow and unless prior information exists suggesting that a particular sky position is likely to contain a pulsar, a FAST drift-scan survey may require a very large amount of observing time before making a discovery[6].

For this paper we chose to examine the likelihood of pulsar discovery in GCs as such clusters are already known to contain relatively large numbers of pulsars, many of which are deemed "interesting." For instance, many such pulsars are fast spinning cases, they are mostly in binary systems and it is possible that the first MSP-black hole binary system will be discovered in a GC (e.g. Clausen et al. 2014). GCs are at known positions, so can be observed with a single FAST observation and their distances/DMs can be estimated from existing data.

The Milky Way Globular Clusters catalog[7] contains 45 GCs that are observable by FAST. The number of potentially-detectable pulsars, N_{psr}, in any given GC depends upon the properties of the cluster. Hui et al. (2010) and Turk & Lorimer (2013) showed that the number of potentially detectable pulsars, N_{psr}, depends mainly upon the stellar interaction rate, Γ, of the cluster

$$N_{\mathrm{psr}} \approx -1.1 + 1.5 \log_{10} \Gamma. \quad (6)$$

[6] We are currently estimating the number of pulsars that could be discovered by such surveys in the early FAST science era. Our results of that analysis will be published elsewhere.

[7] *https://heasarc.gsfc.nasa.gov/db-perl/W3Browse/w3table.pl?tablehead=name=globclust&Action=More+Options*

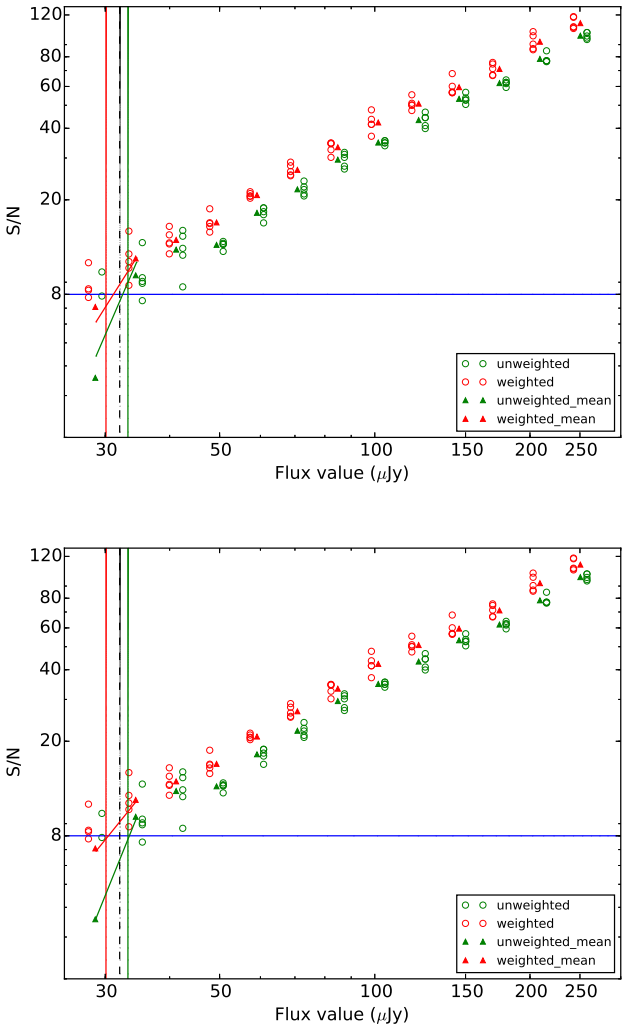

Fig. 3 S/N for a pulsar candidate as a function of flux density value for observations of length 30 s (*top panel*) and 60 s (*bottom panel*). The simulated pulsar has a pulse period of 0.1 s. Five realisations are made for each simulation. The individual results are shown as open circles (red is for the weighted algorithm and green is for the unweighted algorithm). The vertical solid lines indicate the flux density value corresponding to $\mathrm{S/N} = 8$. The vertical dashed line indicates the limiting flux density value presented in Fig. 2.

The 40 GCs in the FAST sky that have measured Γ values[8] are tabulated in Table 3. The first five columns in the table provide the cluster name, right ascension, declination and Galactic coordinates. The "best" estimate of the DM of a pulsar in the cluster is given in column six. If a pulsar is already known in the cluster then this value is taken from the DM of that pulsar (or the mean value for a group of pulsars). If no pulsar is currently known then the Cordes & Lazio (2002) electron density model is used to determine the DM in the direction of the cluster for the assumed distance (listed in column 7). The 8th column lists Γ for each cluster. The number of known pulsars according to the ATNF pulsar catalogue, $N_{\rm known}$, and potential pulsars, $N_{\rm psr}$, as determined from Equation (6) are listed in the 9th and 10th columns respectively.

[8] obtained from *http://data.bao.ac.cn/viz-bin/VizieR?-source=J/ApJ/766/136*

The number of pulsars that may actually be detected, $N_{\rm expect}$, depends upon the sensitivity of the survey and the distance to the GC. Turk & Lorimer (2013) showed that

$$N_{\rm expect} \approx \frac{N_{\rm psr}}{2}\mathrm{erfc}\left(\frac{\log_{10}(S_{\rm min}D^2)-\mu}{\sqrt{2}\sigma}\right), \quad (7)$$

where D is the cluster distance in kpc, $\mu = -1.1$, $\sigma = 0.9$ and $S_{\rm min}$ is in the units of Jy scaled to 1400 MHz. The prediction of $N_{\rm expect}$ thus requires an estimate of $S_{\rm min}$. Our simulations can be used to produce a prediction for $S_{\rm min}$ as a function of the pulse period for each cluster and assumed DM. However, the majority of GC pulsars have millisecond periods. We therefore assume a pulsar with a period of 10 ms. The signal from such pulsars will be significantly smeared in band 1a and so we simply simulate the pulsar in band 1b. This allows us to estimate $S_{\rm min}$ accounting for the cluster position and DM. Of course, these calcula-

Table 3 The 40 GCs in the FAST sky ($-14^\circ \leq \mathrm{Dec} \leq +66^\circ$) that were analysed in this paper. For each cluster we list the equatorial (RA, Dec.) and Galactic (l, b) coordinates, the best estimate of the DM of pulsars in the cluster DM, the distance to the cluster from the Sun (dis), the stellar encounter rate (Γ), the number of currently known pulsars in the cluster ($N_{\rm known}$), the number that a single FAST observation is expected to detect ($N_{\rm expect}$) and the number of observations required to detect one ($N_{\rm drift\_10ms\_1psr}$) or three ($N_{\rm drift\_10ms\_3psr}$) pulsars.

Name	RA (h m s)	Dec (° ′ ″)	l	b	$\mathrm{DM}^1_{\rm best}$ (cm^{-3} pc)	Dis (kpc)	Γ^2	$N_{\rm known}$	$N_{\rm psr}$	$N_{\rm expect}$	$N_{\rm drift\_10ms\_1psr}$	$N_{\rm drift\_10ms\_3psr}$
(1)	(2)	(3)	(4)	(5)	(6)	(7)	(8)	(9)	(10)	(11)	(12)	(13)
NGC 6171	16:32:31.86	–13:03:13.6	3.4	23.0	84.0	6.4	6.77		1	0	≥ 1000	
NGC 6981	20:53:27.70	–12:32:14.3	35.2	32.7	54.7	17.0	4.69		1	0	≥ 1000	
NGC 6517	18:01:50.52	–08:57:31.6	19.2	6.8	180.5⋆	10.6	338	4	15	0	3	40
NGC 6712	18:53:04.30	-08:42:22.0	25.4	–4.3	279.2	6.9	30.8		3	0	≥ 1000	≥ 1000
Pal 11	19:45:14.40	-08:00:26.0	31.8	15.6	124.4	13.4	20.8		2	0	718	
NGC 6539	18:04:49.68	–07:35:09.1	20.8	6.8	186.3⋆	7.8	42.1	1	4	0	30	≥ 1000
IC 1276	18:10:44.20	–07:12:27.4	21.8	5.7	210.1	5.4	7.97		1	0	≥ 1000	
NGC 5634	14:29:37.23	–05:58:35.1	342.2	49.3	32.6	25.2	20.2		2	0	≥ 1000	
NGC 6366	17:27:44.24	–05:04:47.5	18.4	16.0	95.0	3.5	5.14		1	0	≥ 1000	
NGC 6254	16:57:09.05	–04:06:01.1	15.1	23.1	77.4	4.4	31.4		3	0	3	≥ 1000
NGC 6402	17:37:36.10	–03:14:45.3	21.3	14.8	139.6	9.3	124		8	0	5	161
NGC 6218	16:47:14.18	–01:56:54.7	15.7	26.3	72.9	4.8	13.0		2	0	50	
NGC 7089	21:33:27.02	–00:49:23.7	53.4	35.8	45.9	11.5	518		20	1	1	23
Pal 15	16:59:51.00	–00:32:20.0	18.8	24.3	76.9	45.1	0.022†		0			
NGC 6535	18:03:50.51	–00:17:51.5	27.2	10.4	171.7	6.8	0.388		0			
Pal 5	15:16:05.25	–00:06:41.8	0.9	45.9	33.5	23.2	0.002		0			
Pal 3	10:05:31.90	+00:04:18.0	240.1	41.9	42.2	92.5	0.041		0			
NGC 6760	19:11:12.01	+01:01:49.7	36.1	–3.9	199.7⋆	7.4	56.9	2	5	0	18	≥ 1000
NGC 6749	19:05:15.30	+01:54:03.0	36.2	–2.2	193.7⋆	7.9	38.5†	1	4	0	46	≥ 1000
NGC 5904	15:18:33.22	+02:04:51.7	3.9	46.8	29.5⋆	7.5	164	5	9	1	1	49
NGC 6426	17:44:54.65	+03:10:12.5	28.1	16.2	120.7	20.6	1.58		0			
NGC 6934	20:34:11.37	+07:24:16.1	52.1	18.9	82.7	15.6	29.9		3	0	446	≥ 1000
NGC 7078	21:29:58.33	+12:10:01.2	65.0	27.3	66.9⋆	10.4	4510	8	80	5	1	1
Pal 13	23:06:44.44	+12:46:19.2	87.1	42.7	37.7	26.0	0.001		0			
Pal 14	16:11:00.60	+14:57:28.0	28.7	42.2	35.3	76.5	0.002		0			
NGC 7006	21:01:29.38	+16:11:14.4	63.8	19.4	73.7	41.2	9.40		1	0	≥ 1000	
NGC 5053	13:16:27.09	+17:42:00.9	335.7	78.9	25.1	17.4	0.105		0			
NGC 5024	13:12:55.25	+18:10:05.4	332.9	79.8	24.0⋆	17.9	35.4	1	3	0	456	≥ 1000
NGC 4147	12:10:06.30	+18:32:33.5	252.8	77.2	24.1	19.3	16.6		2	0	≥ 1000	
Pal 10	19:18:02.10	+18:34:18.0	52.4	2.7	165.7	5.9	59.0		5	0	4	780
NGC 6838	19:53:46.49	+18:46:45.1	56.7	–4.6	117.0⋆	4.0	2.05†	1	1	0	≥ 1000	
NGC 5272	13:42:11.62	+28:22:38.2	42.2	78.7	26.4⋆	10.2	194	4	10	0	2	95
NGC 5466	14:05:27.29	+28:32:04.0	42.2	73.6	21.7	16.0	0.239		0			
Pal 4	11:29:16.80	+28:58:24.9	202.3	71.8	21.9	108.7	0.019		0			
NGC 6779	19:16:35.57	+30:11:00.5	62.7	8.3	159.0	9.4	27.7		3	0	92	≥ 1000
Pal 2	04:46:05.91	+31:22:53.4	170.5	–9.1	135.7	27.2	929		29	0	15	130
NGC 6205	16:41:41.24	+36:27:35.5	59.0	40.9	30.2⋆	7.1	68.9	5	5	0	3	227
NGC 2419	07:38:08.47	+38:52:56.8	180.4	25.2	66.2	82.6	2.80		1	0	≥ 1000	
NGC 6341	17:17:07.39	+43:08:09.4	68.3	34.9	43.8	8.3	270		13	1	1	8
NGC 6229	16:46:58.79	+47:31:39.9	73.6	40.3	39.2	30.5	47.6		4	0	≥ 1000	≥ 1000

Notes: ⋆ determined from the mean DM of known pulsars in the cluster; † estimates from other properties of the cluster.

tions can be updated for, e.g., much faster spinning pulsars (in which case the sensitivity will be reduced) or for much slower spinning pulsars in which case it would be possible to significantly increase $N_{\rm expect}$ as a wider band would be usable.

$N_{\rm expect}$ is listed in column 11 of the table. We emphasise that these predictions are only estimates, but it is likely that clusters with a large number of expected pulsars are better targets for early FAST observations than those clusters where the expected number of pulsars is zero. These

results represent the likely number of pulsars detectable in a single drift-scan observation. Only four clusters contain a postulated pulsar that could be detected in a single observation. Because these drift-scan observations are short, it will not be difficult to carry out repeated observations of the same cluster. If the telescope can be re-pointed relatively quickly to the cluster then it may be possible to keep the backend system running for multiple observations of the same cluster, allowing for a coherent analysis of the entire data set. However, it will not be trivial to process such complex data sets. More realistically, it is likely that a single observation of a cluster will be made; the backend recording system will then be stopped and later (perhaps hours or days later) another observation will be made of the same cluster. We therefore calculate the number of incoherently added observations that would be necessary to discover around one new MSP. These values are listed in the penultimate column of the table. Equation (7) is a complex function that does not simply scale with the number of observations. In the last column of the table we therefore also presented the number of FAST observations that would be required to detect, on average, three pulsars in each cluster[9], for which the predicted number of pulsars is $\geq$3).

We note that these estimates for the expected number of detections are pessimistic. For instance, we have assumed an S/N cutoff of 8. This is a typical cutoff used for traditional pulsar surveys with long observations. The FAST observations will be relatively short and therefore it is possible that the S/N cutoff could be reduced (hence, decreasing the minimum detectable sensitivity and increasing the number of expected discoveries). Analysing the results from multiple drift-scans will also provide confidence in any candidate. For instance, if a low S/N candidate was observed at the same period and DM in multiple drift-scans then it would likely be a pulsar. In addition, we note that for such short observations it will not be necessary to carry out any acceleration searches and therefore these observations will be significantly more sensitive to pulsars in tight binary systems than previous surveys of GCs that typically used long observations.

In this paper we have applied our drift-scan methodology to an example drift-scan survey of GCs using the FAST telescope. Of course, there are many more types of sources that could be observed. For instance, recent pulsar surveys of Fermi point sources have been extremely productive. Many of these newly discovered pulsars are in eclipsing systems and so it is necessary to carry out multiple observations (separated by many days) for their discovery. The experience gained from carrying out the FAST drift-scan surveys described in this work will also benefit those studies.

5 CONCLUSIONS

For this paper we have:

- Developed a simulation code (which is publicly available for download) to generate single pulse data sets. These data sets are similar to those that will be obtained by FAST in the near future.
- Demonstrated that the lowest part ($270 \sim 560$ MHz) of the early-science receiver band will not be useful for searching for fast MSPs.
- Presented a new channel-weighting scheme for accounting for drift-scans with wide-bandwidth receivers and demonstrated that the detectability of a pulsar with the SIGPROC software increases when using this scheme.
- Carried out trial pulsar searches on the simulated FAST drift-scan data to show that FAST will be able to detect pulsars with a flux density of ~ 40 μJy. This will scale down with the number of drifts as $\frac{1}{\sqrt{N_{\rm drift}}}$.
- Examined expected detections in GCs based on empirical formulae of GC pulsar populations and showed that FAST is likely to detect a few new pulsars in these clusters during the early science period.

We conclude that the FAST telescope will discover pulsars in the early science period, but caution that the 1000s of new discoveries predicted by, e.g., Smits et al. (2009) will require long-duration observations (and hence, the ability to track a source). We emphasise that pulsar searching has traditionally been carried out with single dish telescopes with relatively small fractional bandwidths. The advent of new telescopes, such as the Square Kilometre Array and FAST, and new wide-band receivers for existing telescopes requires that search algorithms are updated in order to maximise the sensitivity of future surveys.

Acknowledgements GH acknowledges the support from the professorship award under the Chinese Academy of Sciences (CAS) President's International Fellowship Initiative (PIFI) in 2015. DL acknowledges the support from the Guizhou Scientific Collaboration Program (No. 20130421). JZ acknowledges the support from the National Natural Science Foundation of China (NSFC, Nos. 11305133 and 11273020). MY acknowledges the support from NSFC (No. Y411101N01). YY acknowledges the support from NSFC (No. 11103045). The NAOC staff acknowledge the support by National Basic Research Program of China (973 program) Nos. 2012CB821800 and 2015CB57100. We also acknowledge grants from NSFC (No. 11373038). We thank the anonymous referee for useful comments on the manuscript.

References

Bates, S. D., Lorimer, D. R., & Verbiest, J. P. W. 2013, MNRAS, 431, 1352

Clausen, D., Sigurdsson, S., & Chernoff, D. F. 2014, MNRAS, 442, 207

Cordes, J. M., & Lazio, T. J. W. 2002, astro-ph/0207156

Deneva, J. S., Stovall, K., McLaughlin, M. A., et al. 2013, ApJ, 775, 51

[9] We chose three pulsars here as a reasonable number to ensure detection in most of the clusters.

Haslam, C. G. T. 1985, Bulletin d'Information du Centre de Donnees Stellaires, 28, 49

Hessels, J. W. T., Ransom, S. M., Kaspi, V. M., et al. 2008, in American Institute of Physics Conference Series, 983, 40 Years of Pulsars: Millisecond Pulsars, Magnetars and More, eds. C. Bassa, Z. Wang, A. Cumming, & V. M. Kaspi, 613

Hobbs, G., Dai, S., Manchester, R. N., et al. 2014, arXiv:1407.0435

Hui, C. Y., Cheng, K. S., & Taam, R. E. 2010, ApJ, 714, 1149

Lorimer, D. 2001, SIGPROC-v1.0: (Pulsar) Signal Processing Programs, Tech. rep., Arecibo Technical Memo

Lorimer, D. R., & Kramer, M. 2004, Handbook of Pulsar Astronomy (Cambridge: Cambridge University Press)

Manchester, R. N., Tuohy, I. R., & Damico, N. 1982, ApJ, 262, L31

Manchester, R. N., Lyne, A. G., Camilo, F., et al. 2001, MNRAS, 328, 17

Manchester, R. N., Hobbs, G. B., Teoh, A., & Hobbs, M. 2005, VizieR Online Data Catalog, 7245

Nan, R., Li, D., Jin, C., et al. 2011, International Journal of Modern Physics D, 20, 989

Smits, R., Lorimer, D. R., Kramer, M., et al. 2009, A&A, 505, 919

Turk, P. J., & Lorimer, D. R. 2013, MNRAS, 436, 3720

Yue, Y., Li, D., & Nan, R. 2013, in IAU Symposium, 291, Neutron Stars and Pulsars: Challenges and Opportunities after 80 Years, ed. J. van Leeuwen, 577

Zhang, L., Wang P., Li, D., et al. 2015, Progress In Astronomy, 33, 506 (in Chinese)